TU Delft

Delft University of Technology

Design of RYSEN

An intrinsically safe and low-power three-dimensional overground body weight support

Plooij, Michaël; Keller, Urs; Sterke, Bram; Komi, Salif; Vallery, Heike; Von Zitzewitz, Joachim

DOI
10.1109/LRA.2018.2812913

Publication date
2018

Document Version
Accepted author manuscript

Published in
IEEE Robotics and Automation Letters

Citation (APA)
Plooij, M., Keller, U., Sterke, B., Komi, S., Vallery, H., & Von Zitzewitz, J. (2018). Design of RYSEN: An intrinsically safe and low-power three-dimensional overground body weight support. *IEEE Robotics and Automation Letters*, *3*(3), 2253-2260. https://doi.org/10.1109/LRA.2018.2812913

Important note
To cite this publication, please use the final published version (if applicable).
Please check the document version above.

Copyright
Other than for strictly personal use, it is not permitted to download, forward or distribute the text or part of it, without the consent of the author(s) and/or copyright holder(s), unless the work is under an open content license such as Creative Commons.

Takedown policy
Please contact us and provide details if you believe this document breaches copyrights.
We will remove access to the work immediately and investigate your claim.

This work is downloaded from Delft University of Technology.
For technical reasons the number of authors shown on this cover page is limited to a maximum of 10.

Author's version
Published in: Robotics and Automation Letters
DOI: 10.1109/LRA.2018.2812913

Design of RYSEN: an Intrinsically Safe and Low-Power 3D Overground Body Weight Support

Michiel Plooij[125], Urs Keller[345], Bram Sterke[2], Salif Komi[3], Heike Vallery[16] and Joachim von Zitzewitz[46]

***Abstract*— BODY weight support (BWS) systems are widely used in gait research and rehabilitation. This paper introduces a new 3D overground BWS system, called the RYSEN[7]. The RYSEN is designed to be intrinsically safe and low power consuming, while still performing at least as well as existing BWS systems regarding human-robot interaction. These features are mainly achieved by decoupling degrees of freedom between motors: slow/high-torque motors for vertical motion and fast/low-torque motors for horizontal motion. This paper explains the design and evaluates its performance on power consumption and safety. Power consumption is expressed in terms of the sum of the positive mechanical output power of all motor axes. Safety is defined as the difference between the mechanical power available for horizontal and vertical movements and the mechanical power that is needed to perform its task. The results of the RYSEN are compared to the performance of three similar systems: a gantry, the FLOAT and a classic cable robot. The results show that the RYSEN and a gantry consume approximately the same amount of power. The amount is approximately half the power consumed by the next best system. For the safety, the gantry is taken as the benchmark, because of its perfect decoupling of directions. The RYSEN has a surplus of 268 W and 126 W for horizontal and vertical movements respectively. This is significantly lower than the next best system, which has a surplus of 1088 W and 1967 W respectively.**

***Index Terms*—Rehabilitation Robotics, Robot Safety**

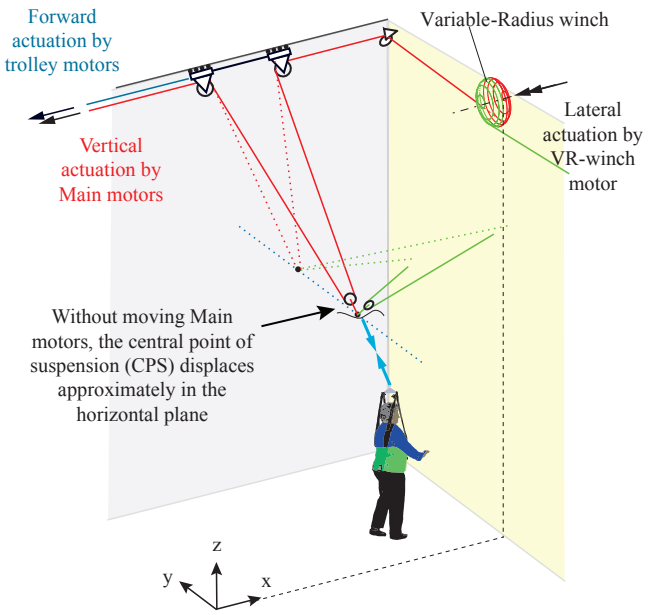

Fig. 1. Simplified mechanical concept of the RYSEN. The figure also depicts the definitions of the coordinate system used in this paper. In this paper we use left to denote the positive y-direction and right to denote the negative y-direction. Similarly, up is the positive z-direction and forward is the positive x-direction.

Manuscript received: Sep, 9, 2017; Revised Dec, 22, 2017; Accepted Feb, 9, 2018.

This paper was recommended for publication by Editor Ken Masamune upon evaluation of the Associate Editor and Reviewers' comments. The work in this paper was partially funded by Eurostars project 10152, and by a Marie-Curie career integration grant PCIG13-GA-2013-618899.

[1] Michiel Plooij and Heike Vallery are with Delft Robotics Institute, Delft University of Technology, Mekelweg 2, 2628 CD Delft, The Netherlands h.vallery@tudelft.nl

[2] Michiel Plooij and Bram Sterke are with Motek, a DIH brand, Hogehilweg 18-C, 1101 CD Amsterdam, The Netherlands michiel.plooij@motekforcelink.com

[3] Urs Keller and Salif Komi are with Center of Neuroprosthetics, Ecole polytechnique federale de Lausanne (EPFL), Campus Biotech H4, Chemin des Mines 9, 1202 Geneva, Switzerland

[4] Urs Keller and Joachim von Zitzewitz are with G-Therapeutics, EPFL Innovation Park, Building C, 1015 Lausanne, Switzerland

[5] Urs Keller and Michiel Plooij should both be considered first author of this paper

[6] Heike Vallery and Joachim von Zitzewitz should both be considered last author of this paper

[7] The content of this paper is part of a patent application. Michiel Plooij and Bram Sterke work (partly) at Motek Medical. Urs Keller, and Joachim von Zitzewitz work (partly) at G-Therapeutics. Both companies benefit from the commercialization of the concepts presented in this paper.

Digital Object Identifier (DOI): see top of this page.

I. INTRODUCTION

ROBOTIC solutions to facilitate gait training have been studied for decades. They can facilitate therapy for individuals who are unable to walk, while relieving physiotherapists of hard physical labor. However, multicenter randomized clinical trials on gait recovery in chronic and subactuate stroke [1, 2] failed to prove substantial advantages in therapeutic outcomes of specific types of robotic gait training compared to other forms of physical therapy. A possible explanation is that the evaluated robotic training constrained users to executing fixed kinematic patterns on a treadmill. In fact, clinical evidence suggests that key ingredients that are needed for neurological recovery are active participation of the patient, including the possibility to make errors [3].

Accordingly, there has been a strong trend in robotic gait training technology towards minimizing intervention during rehabilitation/training for a given user. Compared to early devices, today much more transparent systems are available, such as the Zero-G [4], which supports overground locomotion with only a harness system and a robotic trolley running

© © 2018 IEEE. Personal use of this material is permitted. Permission from IEEE must be obtained for all other uses, in any current or future media, including reprinting/republishing this material for advertising or promotional purposes, creating new collective works, for resale or redistribution to servers or lists, or reuse of any copyrighted component of this work in other works.

on a track on the ceiling. However, the track constrains the system to the sagittal plane. This produces a pendulum-like stabilization effect on the user in lateral direction, which can interfere with the dynamic balancing task [5].

A possible solution was presented by the FLOAT [6], which enables 3D body weight support (BWS) in a large workspace by means of cable robot technology. The device made it possible to investigate the interactions between vertical and horizontal forces during gait, showing that a very precise relative adjustment of these forces is needed to leave gait dynamics unaltered with respect to the unassisted case [7].

However, while freedom of movement of the user has been greatly increased, the power that needs to be installed in the FLOAT to enable its highly dynamic operation has increased as well, requiring extensive safety precautions and stronger electrical installations. The main cause of this is an intrinsic drawback of most parallel robotic systems: coupling of degrees of freedom. The same motors that need to provide the large unloading forces in vertical direction also need to provide the high speeds in horizontal directions to enable gait. Experiments [7] showed that the required horizontal forces are very small in magnitude compared to the vertical ones, while peak speeds in vertical direction are smaller than the ones in horizontal direction. Therefore, the actuators need to be able to generate high torques as well as high speeds, resulting in high power specifications, although the net power transferred to a user is much smaller. This means that during walking, generally one set of motors generates energy, while another set of motors dissipates most of this energy. The resulting motors are heavily over-dimensioned regarding power.

Here, we introduce a new mechanical concept that decouples degrees of freedom almost completely and therefore does not suffer from the above drawbacks, while still enabling dynamic and transparent gait support in 3D (Fig. 1). This concept relies on passive mechanical elements and specific connections of cables in order to decouple degrees of freedom. Without vertical movement and horizontal forces, the concept could even be realized in a fully passive way. This means that the added work that needs to be generated by the actuators is only to enable vertical displacement and to generate small horizontal forces, to compensate for friction or render supportive or resistive forces. This concept has been used for the realization of the gait rehabilitation robot RYSEN, a 3D overground BWS system that is both intrinsically safe and low power.

The rest of this paper starts with a detailed description of the design in section II. Then, an explanation of the methods we used to evaluate the system is given in section III. and section IV shows the evaluation results. The paper ends with a discussion in section V and a conclusion in section VI.

II. The design of the RYSEN

A. Overall mechanical concept

Fig. 2 shows a schematic drawing of the mechanics of the RYSEN. The aim of the design was to split the velocities and forces as much as possible between different motors, leading to a system with low-power motors. In BWS systems, the vertical force is relatively large, but the vertical velocities are relatively low; and horizontal velocities are relatively high, while horizontal forces are rather small. Therefore, our main design philosophy is to split the horizontal directions from the vertical direction, meaning that we want slow, high-torque motors actuating the vertical direction and fast, low-torque motors actuating the horizontal directions. Such a separation of directions could be achieved with a gantry [8, 9], however, such systems have the tendency to be heavyweight, requiring powerful motors to follow a walking human. Cable robots on the other hand, tend to be lightweight [6]. We aim to combine the splitting of directions of gantry robots with the lightweight design of a cable robot. The rest of this section explains the actuation principles in the three Cartesian directions.

B. Posterior-Anterior (x-direction): passive pulleys

For posterior-anterior motion, we use a mechanism that is similar to the Motek Body Weight Support Light [10]. When looking at the left side, the left main cable is guided parallel to a rails and being deflected towards the slingbar by two pulleys that are mounted on a trolley. At the slingbar, a third pulley deflects the cable from one trolley pulley to the other. This mechanism is mirrored on the right side. This makes sure that when moving in posterior-anterior direction, the main motors do not have to move, similar to a gantry system. In order to actuate this direction, both trolleys are actuated by a trolley motor, which can move the trolleys along the rails.

C. Inferior-Superior (z-direction): spring-like behavior

Both the left and the right main cable are directly actuated by a main motor. This motor has to deliver a high force, but it's velocity can be relatively low. Therefore, a worm-wheel transmission of 1:40 is used. This has the additional advantage that the system is self-blocking, meaning that a user is still supported when power is removed from the motors. To simplify the force control and to provide a comfortable stiffness in vertical direction, we used the principle of series elastic actuation [11], with spring stiffnesses of 5kN/m. As shown in Fig. 2, the springs are placed on 180 degrees deflection pulleys of the main cables.

D. Lateral (y-direction): Variable-radius winch

1) Theoretical design: In principle, the lateral direction could have been actuated by the main motors as well. However, this would have resulted in high main motor velocities, much like in the FLOAT [6]. Therefore, there has to be a

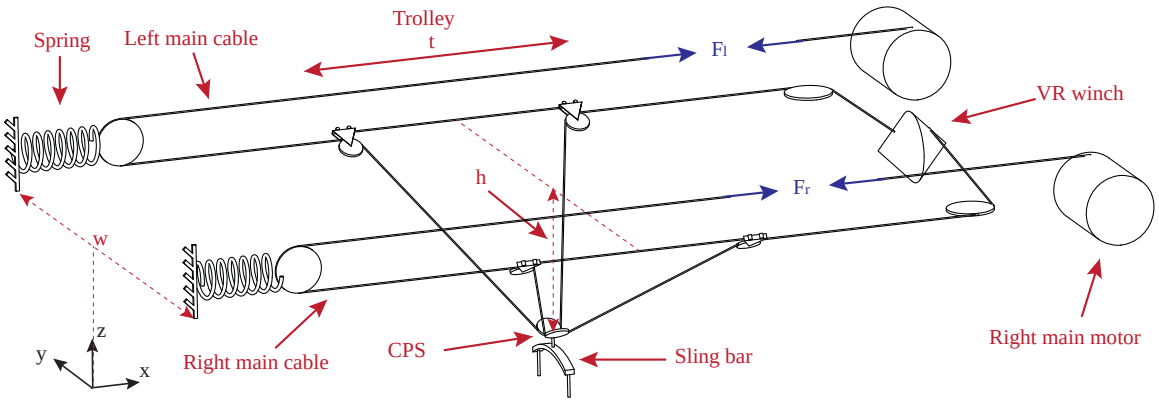

Fig. 2. Schematic drawing of the RYSEN. For clarity of the drawing, the trolley motors that directly actuate the trolleys are left out of the drawing. These trolleys consist of two carts that connect through a cable and move along a rail. The Central Point of Suspension (CPS) is the virtual intersection point of the four cables. A harness worn by a human, can be connected to the sling bar. The left and right main cable both arrive to the Variable Radius winch (VR winch) at the top.

mechanism to transfer cable between the left and the right of the system. An obvious solution would be to have an actuated capstan drum between the two sides. However, this would result in the same problem as the main motors: this capstan motor would have to be fast and deliver a high torque. The high torque is caused by a force difference in the left and right main cable when walking near the left or right edge of the workspace. Therefore, the obvious solution is considered unsafe and consumes too much power.

Instead of a capstan drum, we designed a double-sided variable-radius winch (VR-winch), similar to the mechanism in [12], see Fig. 3. Such a winch allows to choose the radii on both sides (r_l and r_r) as functions of the angular displacement ϕ. In the 1D version in [12], it is possible to create a perfect horizontal end-point trajectory by only rotating the winch, while the winch is always in static equilibrium. In the RYSEN, both the varying vertical position and the varying unloading force (and thus varying spring lengths) make this impossible. Therefore, the rest of this section explains the trade-off that was made in the design of the winch.

Creating a perfect horizontal trajectory by rotating the VR-winch is mainly important in situations where the main motors are already close to their power limits. Otherwise, the main motors can compensate the non-horizontal trajectory. The most extreme situation for the main motors is when walking close to the ceiling with maximum unloading force. The minimum distance from the CPS to the ceiling will be called h_min and the maximum unloading force is $F_\mathrm{z,max}$

In order for the VR-winch to be in torque equilibrium, the following condition should hold:

$$F_\mathrm{l}(y)r_\mathrm{l} + F_\mathrm{r}(y)r_\mathrm{r} = 0 \tag{1}$$

where F_l and F_r are the forces in the left and right main cables and y is the y-position of the CPS. In Eq. (1), both F_l and F_r are functions of y because in order to keep the force acting on the user in y-direction zero, the cable force on the side that the CPS is closest to has to be higher. These functions are given by geometry and the force $F_\mathrm{z,max}$, assuming the desired F_y and F_x are equal to zero. The condition in Eq. (1) can be ensured by making r_l and r_r

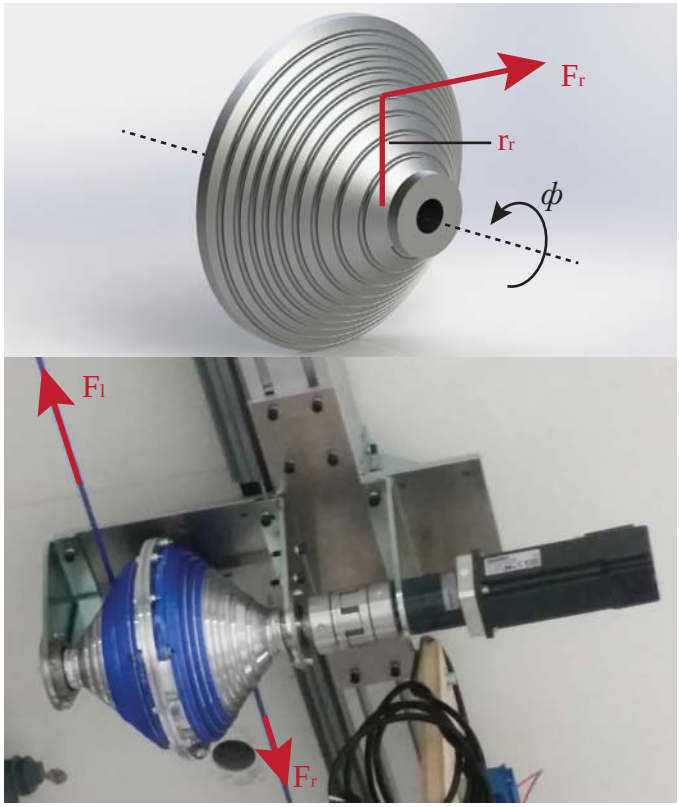

Fig. 3. Render and photograph of the VR-winch. The photograph shows the motor unit of the VR-winch hanging on the ceiling. viewed from the bottom. The ropes are held inside the groove by plastic plates that align with the surface of the winch and are placed on less than a milimeter distance from the rope. In our experience, this is enough to keep the ropes inside their groove.

functions of y like:

$$r_{\mathrm{l}} = r_0 \frac{F_{\mathrm{r}}(y)}{F_{\mathrm{r}}(0)} \tag{2}$$

$$r_{\mathrm{r}} = -r_0 \frac{F_{\mathrm{l}}(y)}{F_{\mathrm{l}}(0)} \tag{3}$$

where r_0 is a design choice that determines the radius of the winch at $y = 0$. Scaling r_0 will result in changing the overall diameter of the winch. Now we define the total length of the cable on the left and right side as C_{l} and C_{r}. This length equals the length of the RYSEN l, minus length of the trolley t, plus twice the length of the cable between the trolley and the CPS. Now from geometry, these values can be calculated as function of y:

$$C_{\mathrm{l}} = l - t + 2\sqrt{(h_{\mathrm{min}})^2 + (\frac{w}{2} - y)^2 + (\frac{t}{2})^2} \tag{4}$$

$$C_{\mathrm{r}} = l - t + 2\sqrt{(h_{\mathrm{min}})^2 + (\frac{w}{2} + y)^2 + (\frac{t}{2})^2} \tag{5}$$

Here w is the width of the system. The length of cable on the left and right side of the VR-winch are denoted by $l_{\mathrm{ow,l}}$ and $l_{\mathrm{ow,r}}$, both change when the VR-winch rotates. In order to create a perfectly horizontal trajectory, the change in cable length on the winch should compensate for the change in cable length on the two sides:

$$l^*_{\mathrm{ow,l}} = l_{\mathrm{ow,0}} - C_{\mathrm{l}}(y) \tag{6}$$

$$l^*_{\mathrm{ow,r}} = l_{\mathrm{ow,0}} - C_{\mathrm{r}}(y) \tag{7}$$

Where the * denotes that this would be the optimal solution when considering only one side. Now unfortunately, conditions (6) and (7) cannot both be met while satisfying Eq.(1). Therefore, we will have to make a trade-off between (6) and (7). In general, the length of cable on a winch is equal to

$$l_{\mathrm{ow}} = \int r \mathrm{d}\phi \tag{8}$$

Differentiating this with respect to ϕ leads to:

$$r = \frac{\mathrm{d}l}{\mathrm{d}\phi} = \frac{\mathrm{d}l}{\mathrm{d}y}\frac{\mathrm{d}y}{\mathrm{d}\phi} \tag{9}$$

Using this, we can derive the derivative of ϕ to y for the left and right side:

$$\left(\frac{\mathrm{d}\phi}{\mathrm{d}y}\right)^*_{\mathrm{l}} = \frac{1}{r_{\mathrm{l}}}\frac{\mathrm{d}l^*_{\mathrm{ow,l}}}{\mathrm{d}y} \tag{10}$$

$$\left(\frac{\mathrm{d}\phi}{\mathrm{d}y}\right)^*_{\mathrm{r}} = \frac{1}{r_{\mathrm{r}}}\frac{\mathrm{d}l^*_{\mathrm{ow,r}}}{\mathrm{d}y} \tag{11}$$

As stated earlier, these two conditions are not equal to each other. Therefore, we have to make a trade-off between them. We do this by realizing that when the system is near the right rail, the left motor generates low torques, while C_{l} changes rapidly when moving laterally. Similarly, when the system is near the left rail, the right motor generates low torques, while C_{r} changes rapidly when moving laterally. Therefore, it makes sense to follow (10) when the CPS is near the right rail and (11) when it is near the left rail. We chose to do this linearly:

$$\mu_{\mathrm{l}} = 1 - \frac{\frac{w}{2} + y}{w} \tag{12}$$

$$\mu_{\mathrm{r}} = \frac{\frac{w}{2} + y}{w} \tag{13}$$

$$\frac{\mathrm{d}\phi}{\mathrm{d}y} = \mu_{\mathrm{l}}\left(\frac{\mathrm{d}\phi}{\mathrm{d}y}\right)^*_{\mathrm{l}} + \mu_{\mathrm{r}}\left(\frac{\mathrm{d}\phi}{\mathrm{d}y}\right)^*_{\mathrm{r}} \tag{14}$$

Finally, we derive ϕ as function of y by integration:

$$\phi(y) = \int \frac{\mathrm{d}\phi}{\mathrm{d}y}\mathrm{d}y \tag{15}$$

The Cartesian positions of the spiral of the VR-winch can now be calculated as follows:

$$y_{\mathrm{w}} = r\cos\phi \tag{16}$$

$$z_{\mathrm{w}} = r\sin\phi \tag{17}$$

$$x_{\mathrm{w}} = r \tag{18}$$

Note that the choice for x_{w} is arbitrary. The choice above ensures a 45-degrees cone shape.

2) Manufacturability considerations: In all equations above, there is nothing that guarantees that this spiral will be manufacturable and usable. Most notably, the winding distance could become smaller than the cable diameter, or even negative. Therefore, we have to check if this happens and correct this, while still obtaining a winch with static equilibria. We call the minimum winding distance d_{min}. The instantaneous winding distance d depends on the rate of change of the x-position of the winding x_{w}, with respect to ϕ. Due to the choice above for a 45-degree cone shape $x_{\mathrm{w}} = r$, so we obtain:

$$d = 2\pi\frac{\partial x_{\mathrm{w}}}{\partial\phi} = 2\pi\frac{\partial r}{\partial\phi} \tag{19}$$

Using Eq. (9), we can rewrite this to

$$d = 2\pi r\frac{\partial r}{\partial y}\frac{\partial y}{\partial l} \tag{20}$$

Now since it should hold that $d \geq d_{min}$, it should hold that

$$\frac{\partial r}{\partial y} \geq d_{min}\frac{1}{2\pi r}\frac{\partial l}{\partial y} \tag{21}$$

If the winch does not comply with this equation at some point, we have to adjust it without compromising torque equilibrium. The solution is to scale r_{l} and r_{r}, such that the above condition is met and the ratio between r_{l} and r_{r} remains the same. So here we assume that a certain winch has been designed that does not suffice the above criterion. We can now constrain the winch as follows:

$$\frac{\partial r_{\mathrm{l}}}{\partial y}_{\mathrm{new}} = \max\left(\frac{\partial r_{\mathrm{l}}}{\partial y}, d_{min}\frac{1}{2\pi r_{\mathrm{l}}}\frac{\partial l}{\partial y}\right) \tag{22}$$

where the $\max$ operator returns the highest value of it's two inputs. From this, we calculate a new r_{l}:

$$r_{\mathrm{l,new}} = \int \frac{\partial r_{\mathrm{l}}}{\partial y}_{\mathrm{new}} \mathrm{d}y \tag{23}$$

Since r_l is also used in the calculation of $\dfrac{\partial r_\mathrm{l}}{\partial y}_{\text{new}}$, this requires looping this procedure until the winding distance is large enough for the whole spiral. Now to keep the ratio between r_l and r_r the same, $r_{\mathrm{r,new}}$ is calculated as

$$r_{\mathrm{r,new}} = r_{\mathrm{l,new}} \frac{r_\mathrm{r}}{r_\mathrm{l}} \tag{24}$$

Finally, we have to recalculate ϕ as function of y, using Eqs. (10)-(15). Similar techniques can be used to bound the winding distance if desired. Using the method described above, r_0 can now be tuned to obtain a VR-winch that is of reasonable size.

III. Evaluation protocol

In this paper, the RYSEN will be evaluated on intrinsic safety and power consumption. The results will be compared with three similar systems (see Fig. 4): a gantry [8, 9], the FLOAT [6] and a classic cable robot with cables extending from the four corners of the room. In the rest of this section, we will first define the metrics we use on safety and power consumption. Secondly, we will describe how we simulated the results for the three similar systems. And finally, we describe the trajectory that is used to evaluate the metrics.

A. Evaluation metrics

We define intrinsic safety of BWS systems as the difference between the end-point mechanical power that is required for its basic functionality, and the end-point mechanical power the system can generate. A lower difference is considered safer, because such a system cannot cause high accelerations. Here we differentiate between power available for horizontal movements and vertical movements. Therefore, for each direction of movement, we calculate the sum of mechanical motor powers, in a worst-case scenario:

$$P_{\mathrm{max},,i} = F_{\mathrm{max}}^T J_i v_{\mathrm{max}} \tag{25}$$

where $F_{\mathrm{max}}$and v_{max} are vectors containing the maximum motor forces and maximum motor velocities during operation and J_i is a diagonal matrix defining the worst-case scenario for the direction i, i.e. the x, y or z direction. Since the system under consideration is a cable robot, J_i is chosen such that the cables can only insert power in tension. For minimal required mechanical power, we take the gantry system as a benchmark, because it perfectly decouples the Cartesian directions.

There are many metrics that can be used for the power consumption of robots, as noted in [13]. The metrics mainly differ with respect to electrical losses and negative motor power. Here we assume that negative motor power is dissipated and we discard motor losses such as copper losses and gearbox friction. The latter makes comparison between BWS system easier, because the mechanical power does not depend on the specific actuator that was chosen. These choices are further discussed in section V. The resulting power is thus equal to:

$$P_{\mathrm{peak}} = \sum_j \max(F_j v_j, 0) \tag{26}$$

where F is the motor force, v is the motor velocity, j denotes the motor number and the max function returns the maximum of the two inputs. In the results, we will also show the forces and velocities separately.

B. Simulation of the other three systems

The hardware results of RYSEN will be compared to simulation results of a gantry system, the FLOAT and a classic cable robot. Therefore, reasonable estimates are required for the motor velocities and forces of those systems performing the same task.

As an estimate of the velocities of the gantry motors, we use the velocity of the CPS of the RYSEN. As an estimate of the gantry motor forces, we take the forces being applied to the CPS. However, this neglects the fact that gantry systems are more heavyweight and thus need force to accelerate the system itself. We estimated reasonable masses for a gantry system to be 5 kg in y-direction and 20 kg in x-direction (see Fig. 1 for definitions of x, y, and z and left and right). These masses, multiplied by the accelerations, are added to the CPS forces mentioned above.

For the velocities of the FLOAT, we calculated the four cable lengths that the FLOAT would have from the winches to the node. In the FLOAT, the node is the point where the four cables are joined (see Fig. 4c), in contrast to the use of pulleys at the CPS of the RYSEN. The time derivative of these cable lengths gives the motor velocities. In the FLOAT, the four motors have to generate the force for all three Cartesian directions. Therefore, we estimated the motor forces of the FLOAT as consisting of two parts. The first part is the main cable force, which is equal to the main cable force of the RYSEN. The second part is the force of the trolley motors in the RYSEN, that in the FLOAT would have to be applied by the four motors. We assume that this force of the left trolley motor splits 50/50 over the two FLOAT motors on the left side and assume the same for the right side.

The velocities of the classic cable robot motors are calculated similarly to the velocities of the FLOAT: differentiating the Euclidian distance between the corners of the room and the CPS. The motor forces are obtained by optimizing the cable tensions such that the norm of the cable tensions is minimized, the resulting force is equal to the CPS force of the RYSEN and the cable tensions have a minimum value of 50 N to prevent the cable from going slack.

C. System parameter choices and Evaluation trajectory

The RYSEN we used for the evaluation in this paper has a length of 10 m (x-direction), width of 2.7 m (y-direction) and height of 3.3 m (z-direction). The evaluation is performed by suspending a sand bag of 20 kg on the sling bar. We designed a trajectory that resembles the characteristics of

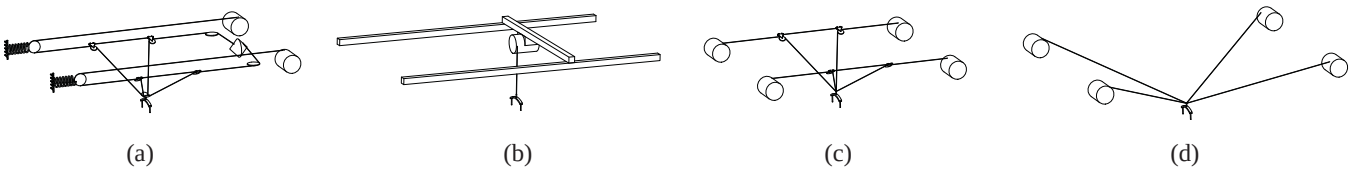

Fig. 4. The four systems compared in this paper: (a) the RYSEN, (b) a gantry, which is basically an x-y-z robot, (c) the FLOAT, which has four large motors that connect to four cables. The four cables are deflected by pulleys on a trolley and are joined in a node just above the sling bar and (d) a classic cable robot that has no pulleys or trolleys. The cables directly run from the four motors to a node above the sping bar. System (b)-(d) are simulated.

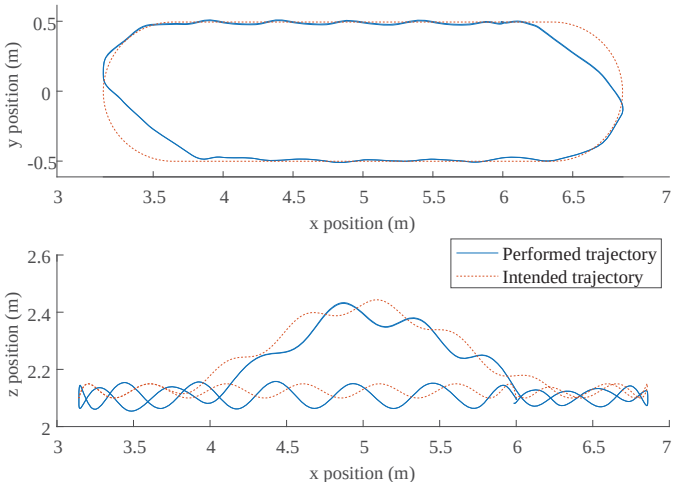

Fig. 5. The trajectory of the CPS in Cartesian space. This trajectory is followed in counterclockwise direction with a velocity of 1 m/s in horizontal direction and an unloading of 20 kg.

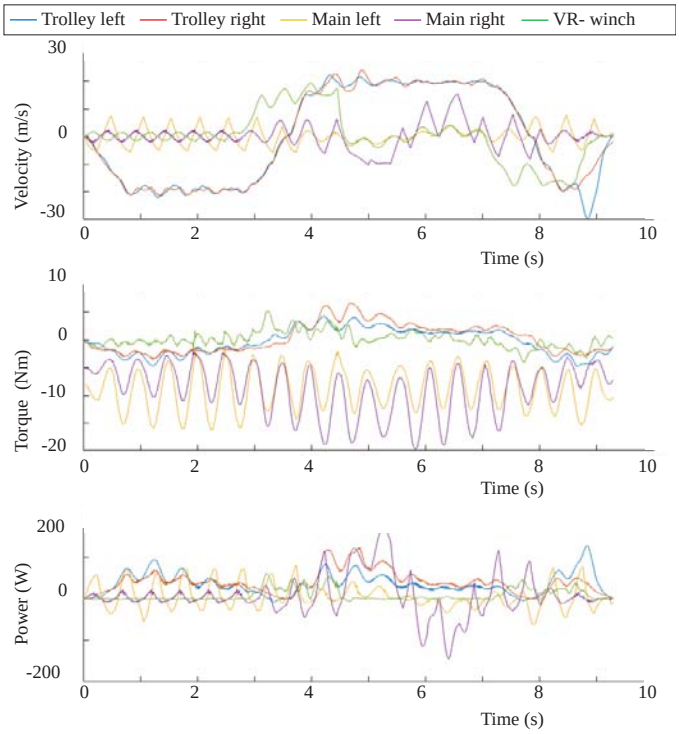

Fig. 6. The velocities, forces and mechanical power consumption of the five motors of the RYSEN.

normal walking. It consists of six phases: 1. an acceleration phase of 1.4 m/s^2 in negative x-direction, 2. constant velocity of 1m/s in negative x-direction, 3. turning 180 degrees with a radius of 0.5m, 4. constant velocity of 1m/s in positive x-direction, 5. turning 180 degrees with a radius of 0.5m and 6. decelerating with 1.4 m/s^2. During phase 4, a stair-walking task is simulated with a sinusoidal profile, in which the vertical CPS position increases and decreases by 0.3m in a total of 2 seconds. During all phases, a vertical oscillation with an amplitude of 5cm and a frequency of 2Hz is added to the trajectory. This trajectory is followed using a feedforward position controller in motor space, assuming infinitely stiff springs (see Fig. 5). Due to the main springs, it is to be expected that the intended trajectory described above will not be followed accurately. This is acceptable as long as the resulting trajectory is qualitatively similar to the intended trajectory. The experiment is repeated three times and the results are averaged.

IV. Results

This section shows the results of the hardware experiments we performed on the RYSEN and the simulated results for the systems in Fig. 4b-4d. Fig. 5 shows the trajectory of the CPS. This trajectory was followed in counterclockwise direction with a horizontal speed of 1 m/s.

Fig. 6a and 6b show the velocities and the torques of the motors respectively. These two graphs show the splitting of velocities and torques between motors in the RYSEN. The trolley motors and VR-winch motor have a relatively high velocity, but a low torque. The main motors on the other hand have a relatively low velocity, but high torques. This leads to the graph in Fig. 6c, which shows the mechanical output power of the motors over time. This graphs show that none of the motors has a peak power that exceeds 170W.

Fig. 7 shows a comparison of the mechanical output power over time for four systems: the RYSEN, a gantry, the FLOAT and a classic cable robot, whereby the latter three are simulation results. Table I summarizes the results for the metrics on power consumption and safety, as defined in section III. The first column shows what was also displayed in Fig. 7: the peak power consumptions of the RYSEN and a gantry system are similar. The peak power consumption of the FLOAT is 1.92 times that of the RYSEN. The classic cable robot in turn has a peak power that is 1.98 times that

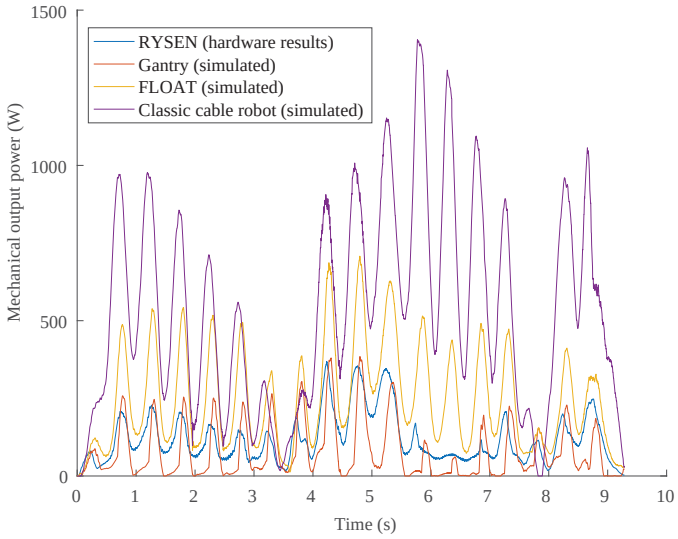

Fig. 7. The power consumptions of the four systems over time.

TABLE I
SUMMARY OF THE RESULTS. THIS TABLE LISTS THE PEAK POWER DURING THE TASK (P_{PEAK}), THE MECHANICAL POWER AVAILABLE FOR HORIZONTAL MOVEMENT (P_{H}) AND THE MECHANICAL POWER AVAILABLE FOR VERTICAL MOVEMENT (P_{V})

System	P_{peak}	P_{h}	P_{v}
RYSEN	368 W	403 W	606 W
Gantry (simulated)	385 W	135 W	480 W
FLOAT (simulated)	708 W	1223 W	2247 W
Classic cable robot (simulated)	1405 W	2601 W	5203 W

of the FLOAT.

We defined safety in terms of the surplus of power available for horizontal and vertical movement. For this metric, the gantry can be seen as the benchmark, because it perfectly decouples the three Cartesian directions. This means that the values for the available horizontal and vertical power as shown in Table I can be regarded as the absolute minima for this task. The table further shows that the RYSEN has a surplus of 268 W for horizontal movement and 126 W for vertical movement. This is significantly lower than the power surplus of the FLOAT (1088 W and 1967 W respectively) and a classic cable robot (2022 W and 4722 W respectively).

V. DISCUSSION

This section discusses the performance results, other metrics that were not discussed so far, the used power metric and tracking errors in the hardware results.

A. Power results

Table I shows the power consumptions of the four compared systems. It shows that the power consumption of a classic cable robot is 1.98 times that of the FLOAT, which in turn is 1.92 times that of the RYSEN. The absolute vales of the powers are still relatively low, i.e. 1405 W, 708 W and 368 W respectively. However, since this is the mechanical power consumption, the electrical power consumption will be a multiple of this. The power consumption of BWS systems is mainly important because of room requirements. When the electrical power consumption stays below 3680 W, it is possible to connect the system to a one phase line of 230 V times 16 A, which is commonly available in hospitals and research centers. If more power would be needed, a three-phase power line would have to be installed, which is typically expensive and time-consuming. A preliminary study we performed shows that the RYSEN can perform all tasks typically performed with BWS systems (i.e. walking, stair climbing, turning etc.) with an unloading force of 90 kg and an electrical power consumption below 3680 W.

B. Safety results

The results on the safety metric show that the RYSEN has a surplus of power for horizontal movement of 268 W. This corresponds to accelerating a mass of 50 kg to 2 m/s in 0.37 s, which is twice as large as the reaction time of humans [14, 15]. For the FLOAT, the acceleration time equals 0.09 s and for a classic cable robot this equals only 0.05 s. For the vertical movement, the surplus of power of the RYSEN is 126 W. This corresponds to lifting a 50 kg mass with a velocity of 0.26 m/s. For the FLOAT this velocity equals 4.01 m/s and for a classic cable robot even 9.63 m/s.

For the safety of a system, intrinsic safety is not a prerequisite. In the end, safety depends on the combination of the mechanical, electrical and software design. This includes safety logic, drive limitations and signal monitoring in the controller. However, we believe that the less a system is even capable of hurting a human, the safer the system will be in the end. The results in this paper show that the RYSEN scores significantly better on intrinsic safety than the FLOAT and a classic cable robot.

C. Other performance metrics

This paper compared different systems on safety and power consumption. Although being important, there are other performance metrics that were not discussed. The most important remaining performance metric is the human-robot interaction. At the very least, a BWS system has to be able to execute movements a person is likely to perform. For the RYSEN this basic performance was shown in this paper. Additionally, the interaction force has to coincide with a desired force, depending on the type of training. Showing the transparency of the RYSEN is part of future work.

When ignoring transparency, the results in this paper suggest that a gantry system would be as good as the RYSEN. However, a gantry system has significantly more inertia, making its response slower. Therefore, we expect cable robots such as the FLOAT and the RYSEN have a higher transparency than gantry systems. Furthermore, the mass of gantry systems increase with their span, while cable robots don't suffer from such scaling issues.

D. The used power metric

As mentioned in section III, there are many possible metrics for the power consumption of robots. There are two choices made in the metric we used. First, we chose mechanical output power instead of mechanical motor power or electrical power. The justification of this choice is that this metric does not depend on any specific actuator choice. This means that the conclusions will still hold when available actuator technology changes. This choice neglects the main motor losses, which are gearbox friction and copper losses. Frictional losses are typically dominant with high transmission ratios between motors and joints and copper losses are dominant with low transmission ratios. Both of these losses typically scale approximately quadratically with the mechanical power. Therefore, we expect that the additional losses will scale approximately equally for all systems. The second choice we made was assuming that negative power is dissipated on an axis level. Although the drives of the RYSEN allow for electrical power transfer between axes, this power transmission is inefficient due to frictional and copper losses that are intrinsic to using the motors as generators.

E. Tracking errors

Fig. 5 shows that there are two types of tracking errors. First, the tracking error in the corners is caused by the methods we used: the RYSEN has to accelerate the 20 kg mass in horizontal direction, while it is designed to only apply small horizontal forces. When used as a BWS, the system does not have to accelerate the user itself, meaning that the tracking error in these results is not an issue. Secondly, there is a phase shift between the intended trajectory and the performed trajectory. This is caused by the controller we used: a feedforward position controller in motor space, assuming infinitely stiff springs. Due to the main springs, tracking errors occur. Since the trajectories are qualitatively similar and tracking error is not used as outcome measure, the conclusions of this paper are not affected.

VI. Conclusions

This paper presented the mechanical concept of the RYSEN and compared its power consumption and safety to three similar systems: a gantry, the FLOAT and a classic cable robot. We first conclude that the power consumptions of the RYSEN is similar to that of a gantry system and approximately half of that of the FLOAT. Secondly, for the exemplary task we implemented, the surplus of mechanical power of the RYSEN is 268 W for horizontal movement and 126 W for vertical movement. Compared to the FLOAT (1088 W and 1767 W respectively) and a classical cable robot (2022 W and 4722 W respectively), we conclude that the RYSEN is intrinsically safe. The low power consumption and intrinsic safety make the RYSEN a safe body weight support system that even has the potential to run on a single-phase of electric power.

References

[1] J. Hidler *et al.*, "Multicenter randomized clinical trial evaluating the effectiveness of the lokomat in subacute stroke." *Neurorehabilitation and Neural Repair*, vol. 23, no. 1, pp. 5–13, 2009.

[2] T. G. Hornby *et al.*, "Enhanced gait-related improvements after therapist- versus robotic-assisted locomotor training in subjects with chronic stroke: a randomized controlled study." *Stroke*, vol. 39, no. 6, pp. 1786–1792, Jun 2008.

[3] A. Pennycott *et al.*, "Towards more effective robotic gait training for stroke rehabilitation: a review," *J. of neuroeng. Rehabil.*, vol. 9, no. 1, p. 65, 2012.

[4] J. Hidler *et al.*, "ZeroG: overground gait and balance training system." *J Rehabil Res Dev*, vol. 48, no. 4, pp. 287–298, 2011.

[5] A. Pennycott *et al.*, "Effects of added inertia and body weight support on lateral balance control during walking," in *Proc. of the IEEE Int. Conf. on Rehabilitation Robotics*. IEEE, 2011, pp. 1–5.

[6] H. Vallery *et al.*, "Multidirectional Transparent Support for Overground Gait Training," in *Proc. of the IEEE Int. Conf. on Rehabilitation Robotics*, 2013, pp. 1–7.

[7] J.-B. Mignardot *et al.*, "Multidirectional gravity-assist algorithm that enhances locomotor control after neurological disorders," *Science Translational Medicine*, no. 9, 2017.

[8] D. Shetty *et al.*, "Ambulatory suspension and rehabilitation apparatus," 2008, uS Patent 7,462,138.

[9] NASA, "Active Response Gravity Unload System," https://www.nasa.gov/centers/johnson/engineering/integrated_environments/active_response_gravity/, [Online; accessed 24-August-2017].

[10] a. D. b. Motek, "C-Mill — Motekforce Link," https://www.motekforcelink.com/product/c-mill/, [Online; accessed 8-September-2017].

[11] G. A. Pratt and M. M. Williamson, "Series elastic actuators," in *Intelligent Robots and Systems, IEEE/RSJ Int. Conf. on*, vol. 1. IEEE, 1995, pp. 399–406.

[12] S. Seriani and P. Gallina, "Variable radius drum mechanisms," *Journal of Mechanisms and Robotics*, vol. 8, no. 2, p. 021016, 2016.

[13] T. Verstraten *et al.*, "Optimizing the power and energy consumption of powered prosthetic ankles with series and parallel elasticity," *Mechanism and Machine Theory*, vol. 116, pp. 419 – 432, 2017.

[14] S. Thorpe *et al.*, "Speed of processing in the human visual system," *Nature*, vol. 381, no. 6582, pp. 520–522, 1996.

[15] P. Cordo *et al.*, "Proprioceptive coordination of movement sequences: role of velocity and position information," *J. Neurophysiol.*, vol. 71, no. 5, pp. 1848–1861, 1994.